Electronic Supplementary Material (ESI) for Journal of Materials Chemistry C.
This journal is © The Royal Society of Chemistry 2022

Z-scheme photocatalytic solar-energy-to-hydrogen conversion driven by the HfS_2/SiSe heterostructure

Chun-Fang Zhang, Chuan-Lu Yang *, Mei-Shan Wang, and Xiao-Guang Ma

School of Physics and Optoelectronic Engineering, Ludong University, Yantai 264025, China

1. tructural and electronic properties of HfS_2 and SiSe monolayer and HfS_2/SiSe heterostructure

Table S1 The lattice parameters and bandgaps of the HfS_2 and SiSe monolayers (primitive cell). The previously reported data are also included.

configurations	*a* (Å)	Bandgap (eV)
HfS_2(present)	3.62	2.01
HfS_2[1]	3.64	1.12*
HfS_2[2]	3.68	2.05
HfS_2(H-phase)[3]	3.54	1.95
HfS_2[4]	3.53	1.72
HfS_2[5]	3.61	1.99
SiSe(present)	3.49	2.18*, 2.96
SiSe[6]	3.52	2.12*
SiSe[7]	3.55	3.03

* Results obtained using PBE calculations

* Corresponding author. *E-mail address:* ycl@ldu.edu.cn. (C.L. Yang).

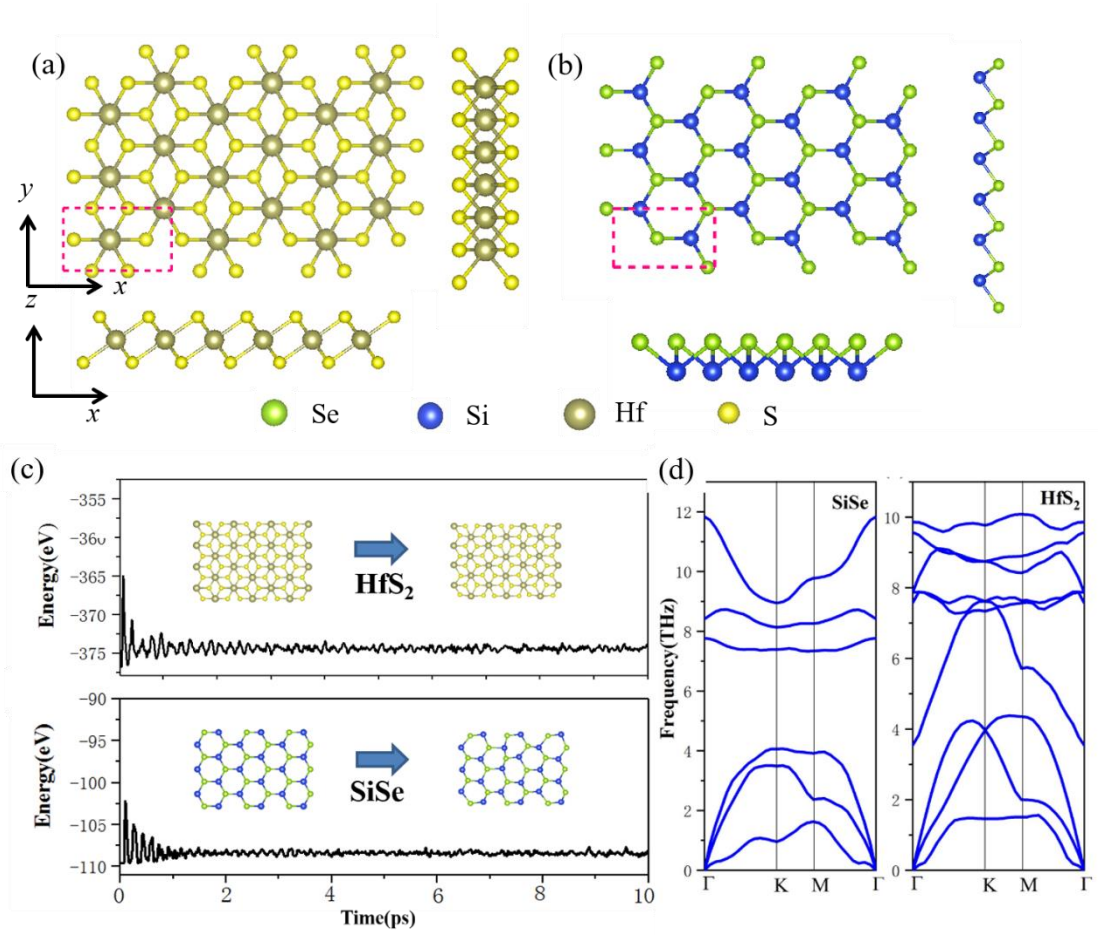

Fig. S1. (a)-(b) Top and side views of the HfS_2 monolayer and SiSe monolayers, (c) The results of the AIMD simulation within 10 picoseconds at 400 K. (d) Phonon dispersions.

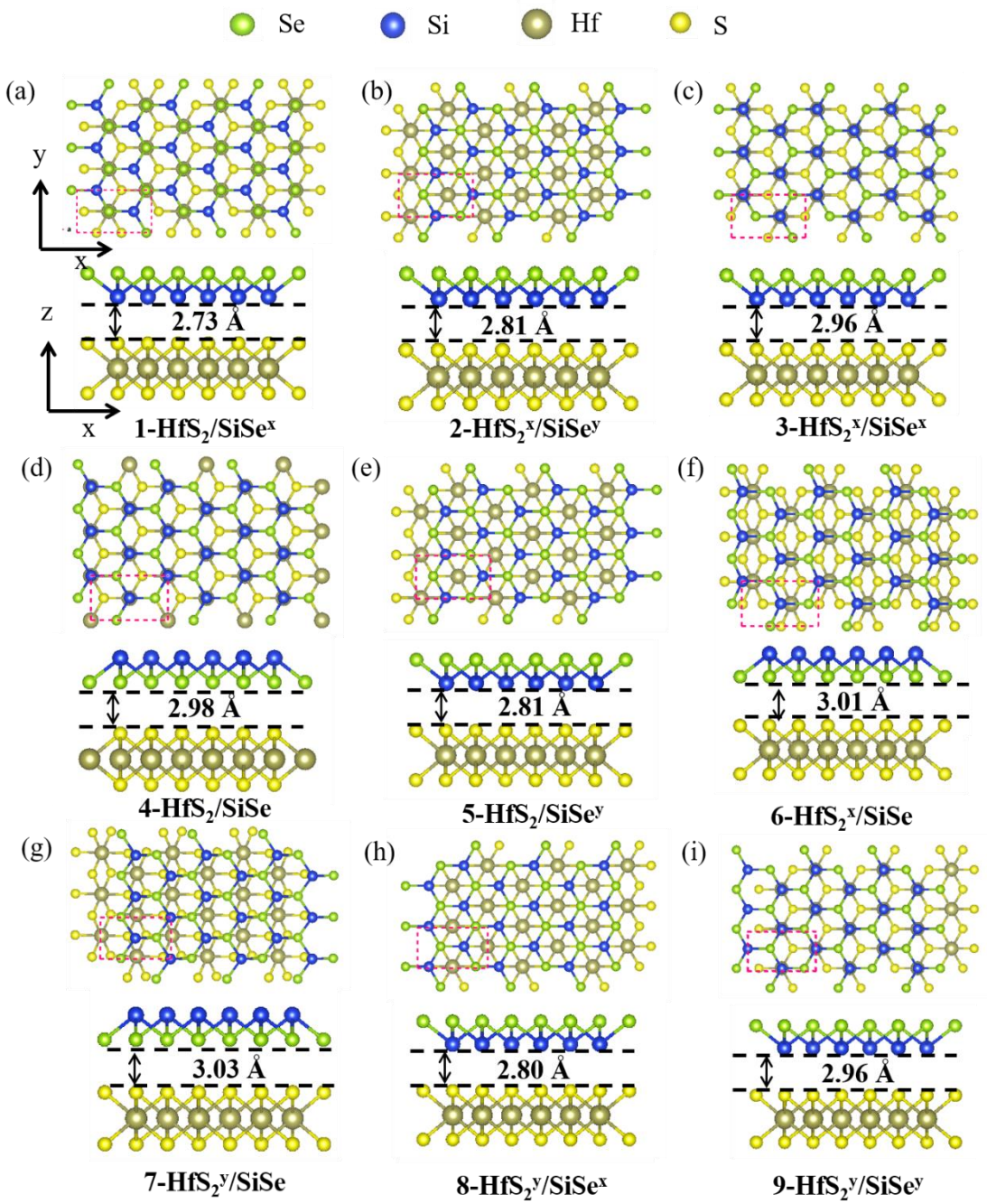

Fig. S2. The geometrical structures for all considered configurations of the HfS_2/SiSe heterostructure.

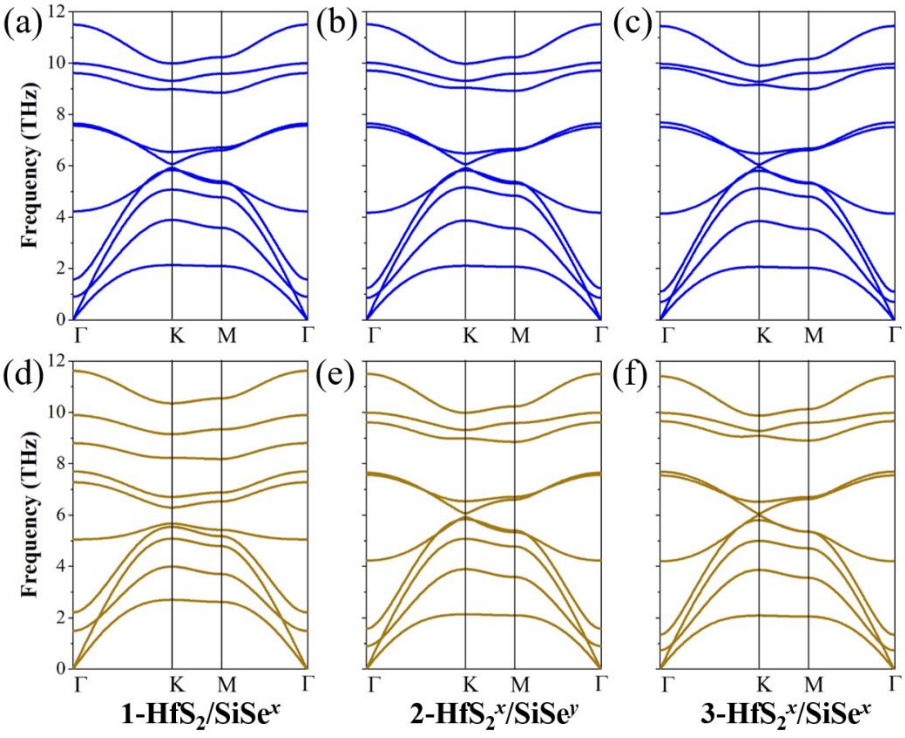

Fig. S3. The Phonon dispersion of three configurations. (a-c) phonon dispersion without considering a solvent effect, (c-d) phonon dispersion with solvent effect.

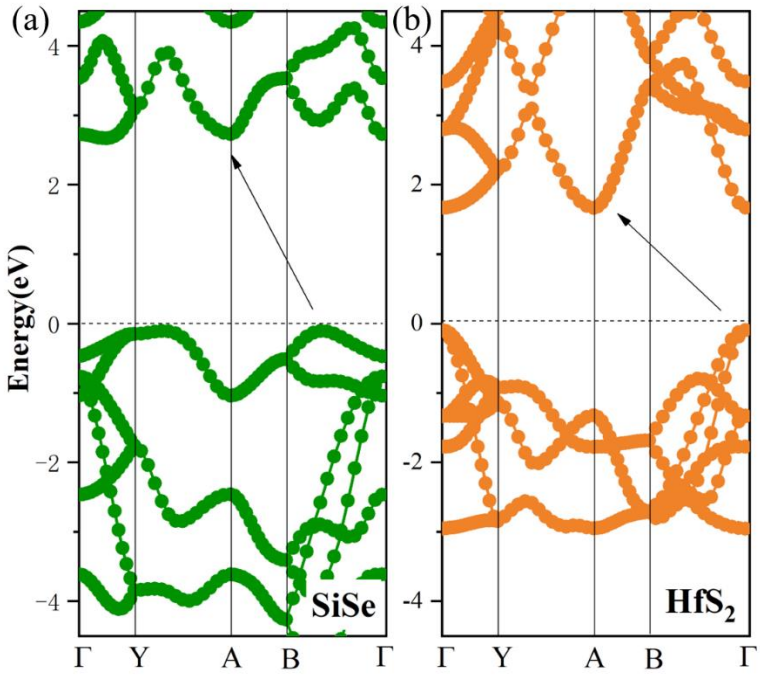

Fig. S4. Band energy structures of the separated HfS_2 and SiSe monolayers.

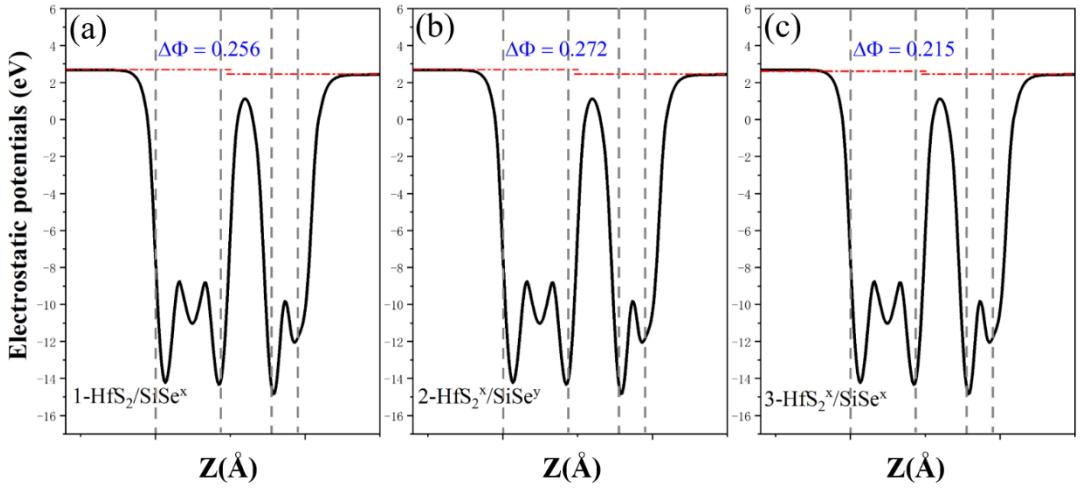

Fig. S5. The electrostatic potentials and the differences of the vacuum energy levels ($\Delta\Phi$).

2. Calculation formula and details of current-carrying mobility

The formula can be obtained from the deformation potential theory:[8]

$$\mu = \frac{2e\hbar^3 C}{3K_B T m^{*2} E_d^2} \qquad (6)$$

In the formula, C is the elastic modulus, E_d is DP constant, m^* is effective mass $\hbar$ is Jowah Planck's constant, K_B is Boltzmann's constant, T for the temperature.

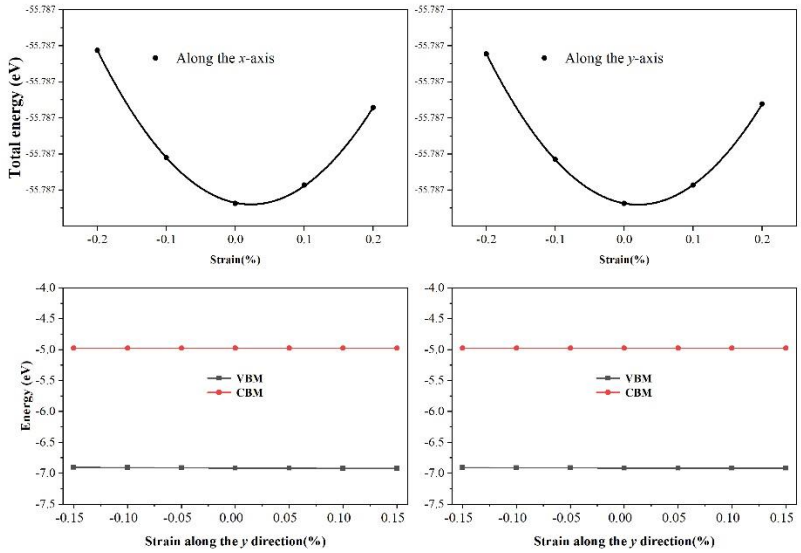

Fig. S6. (a-b) The curves for fitting the effective masses, and (c-d) The shifts of CBM/VBM for fitting the deformation potential constants for the HfS_2 monolayer.

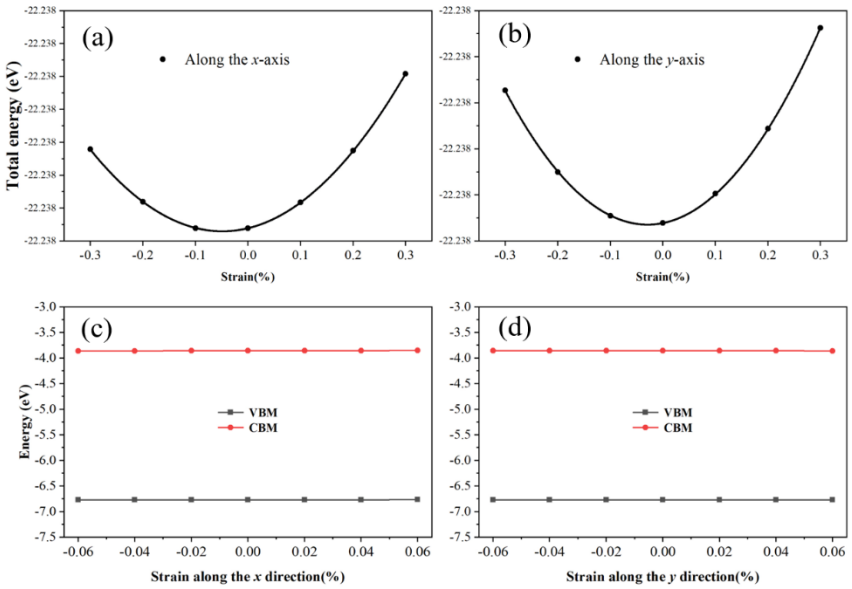

Fig. S7. (a-b)The curves for fitting the effective masses, and (c-d) The shifts of CBM/VBM for fitting the deformation potential constants for the SiSe monolayer.

Table S2 The carrier mobilities of the HfS_2 and SiSe monolayers.

configurations	Carrier type		m^* (/m_0)	C_x (N/m)	C_y (N/m)	E_d^x (eV)	E_d^y (eV)	μ_x (cm^2/ V.s)	μ_y (cm^2/ V.s)
HfS_2	tensile	electron	0.47	123.30	123.83	0.30	0.82	8.81×10^4	1.12×10^4
		hole	0.47	123.30	123.83	1.18	1.18	5.69×10^3	5.72×10^3
	compressive	electron	0.47	123.30	123.83	0.30	0.82	8.81×10^4	1.12×10^4
		hole	0.47	123.30	123.83	6.35	6.87	1.97×10^2	1.69×10^2
SiSe		electron	0.70	61.16	60.92	6.59	3.89	41.18	2.09×10^3
		hole	1.54	61.16	60.92	3.72	1.34	26.34	1.22×10^3

3. The details of the calculational method and results of solar-energy-to-hydrogen（SETH）conversion efficiency

According to the calculational methodology of SETH conversion efficiency (η_{SETH}) proposed by Fu *et* al.,[9] $P(h\omega)$ is the expression for the AM 1.5G solar energy flux by the photon energy $h\omega$, band gaps E_g(HSE) is the largest band gap between two monolayers. The energy conversion efficiency of light absorption is defined as η_{abs}, the efficiency of carrier utilization is defined as η_{cu}, SETH conversion efficiency is defined as η_{STH}, and corrected SETH efficiency of photocatalytic water splitting is defined as η. Then, the calculational expressions are as follows:

$$\eta_{SETH} = \eta_{abs} \times \eta_{cu} \quad (1)$$

$$\eta_{abs} = \frac{\int_{E_g}^{\infty} P(h\omega)d(h\omega)}{\int_0^{\infty} P(h\omega)d(h\omega)} \quad (2)$$

$$\eta_{cu} = \frac{\Delta V \int_{E_g}^{\infty} \frac{P(h\omega)}{h\omega} d(h\omega)}{\int_{E_g}^{\infty} P(h\omega)d(h\omega)} \quad (3)$$

$$E=\begin{cases} E_g, (x(\mathrm{H_2})\geq 0.2, x(\mathrm{O_2})\geq 0.6) \\ E_g+0.2-x(\mathrm{H_2}), (x(\mathrm{H_2})<0.2, x(\mathrm{O_2})\geq 0.6) \\ E_g+0.6-x(\mathrm{O_2}), (x(\mathrm{H_2})\geq 0.2, x(\mathrm{O_2})<0.6) \\ E_g+0.8-x(\mathrm{H_2})-x(\mathrm{O_2}), (x(\mathrm{H_2})<0.2, x(\mathrm{O_2})<0.6) \end{cases} \quad (4)$$

$$\eta=\eta_{SETH}\times\frac{\int_0^\infty P(h\omega)d(h\omega)}{\int_0^\infty P(h\omega)d(h\omega)+\Delta\Phi\int_0^\infty\frac{P(h\omega)}{h\omega}d(h\omega)} \quad (5)$$

Where $\Delta\Phi$ is the difference between the vacuum energy levels. ΔV is the potential difference of 1.23 eV for water splitting, and E is the energy of photons for water splitting. $x(\mathrm{H_2})$ and $x(\mathrm{O_2})$ are the over-potentials for HER and OER.

Table S3 The overpotentials and η for the ZS-I scheme of 1-HfS_2/$SiSe^x$.

Configuration	$x(H_2)$(eV)	$x(O_2)$ (eV)	E_g(HSE)	$\triangle\Phi$(eV)	η(%)
4%	1.16	1.52	2.40	0.13	9.51
3%	1.11	1.46	2.41	0.04	9.42
2%	1.02	1.40	2.38	0.06	9.84
1%	0.97	1.33	2.39	0.16	9.62
0	0.91	1.25	2.40	0.26	9.41
-1%	0.90	1.17	2.45	0.36	8.61
-2%	0.84	1.08	2.46	0.45	8.41
-3%	0.79	0.99	2.47	0.55	8.15

Table S4 The overpotentials and η for the ZS-II scheme of 1-HfS_2/$SiSe^x$.

Configuration	$x(H_2)$(eV)	$x(O_2)$ (eV)	E_g(HSE)	$\triangle\Phi$(eV)	η(%)
4%	1.03	1.65	2.40	0.13	9.51
3%	1.08	1.50	2.41	0.04	9.42
2%	1.08	1.34	2.38	0.06	9.84
1%	1.13	1.17	2.39	0.16	9.62
0	1.17	0.99	2.40	0.26	9.41
-1%	1.25	0.81	2.45	0.36	8.61
-2%	1.30	0.63	2.46	0.45	8.41
-3%	1.34	0.44	2.47	0.55	6.04

Table S5 The overpotentials and η for the ZS-III scheme of 1-HfS_2/$SiSe^x$.

Configuration	$x(H_2)$(eV)	$x(O_2)$ (eV)	E_g(HSE)	$\triangle\Phi$(eV)	η(%)
4%	1.03	1.52	2.40	0.13	9.51
3%	1.08	1.46	2.41	0.04	9.42
2%	1.08	1.40	2.38	0.06	9.84
1%	1.13	1.33	2.39	0.16	9.62
0	1.17	1.25	2.40	0.26	9.41
-1%	1.25	1.17	2.45	0.36	8.61
-2%	1.30	1.08	2.46	0.45	8.41
-3%	1.34	0.99	2.47	0.55	8.15

Table S6 The overpotentials and η for the ZS-IV scheme of 1-HfS_2/$SiSe^x$.

Configuration	$x(H_2)$(eV)	$x(O_2)$ (eV)	E_g(HSE)	$\triangle\Phi$(eV)	η(%)
4%	1.16	1.65	2.40	0.13	9.51
3%	1.11	1.50	2.41	0.04	9.42
2%	1.02	1.34	2.38	0.06	9.84
1%	0.97	1.17	2.39	0.16	9.62
0	0.91	0.99	2.40	0.26	9.41
-1%	0.90	0.81	2.45	0.36	8.61
-2%	0.84	0.63	2.46	0.45	8.41
-3%	0.79	0.44	2.47	0.55	6.04

Table S7 The overpotentials and η for the ZS-I scheme of 2-HfS_2^x/$SiSe^y$.

Configuration	$x(H_2)$(eV)	$x(O_2)$ (eV)	E_g(HSE)	$\triangle\Phi$(eV)	η(%)
4%	0.90	1.50	2.29	0.08	11.48
3%	0.86	1.38	2.30	0.01	11.41
2%	0.82	1.33	2.31	0.10	11.07
1%	0.78	1.27	2.33	0.19	10.67
0	0.74	1.19	2.35	0.27	10.20
-1%	0.70	1.11	2.37	0.36	9.83
-2%	0.67	1.02	2.39	0.44	9.41
-3%	0.66	0.92	2.44	0.53	8.65

Table S8 The overpotentials and η for the ZS-II scheme of 2-HfS_2^x/$SiSe^y$.

Configuration	$x(H_2)$(eV)	$x(O_2)$ (eV)	E_g(HSE)	$\triangle\Phi$(eV)	η(%)
4%	0.83	1.58	2.29	0.08	11.48
3%	0.87	1.37	2.30	0.01	11.41
2%	0.92	1.24	2.31	0.10	11.07
1%	0.96	1.08	2.33	0.19	10.67
0	1.01	0.92	2.35	0.27	10.20
-1%	1.06	0.75	2.37	0.36	9.83
-2%	1.11	0.57	2.39	0.44	8.99
-3%	1.19	0.39	2.44	0.53	5.78

Table S9 The overpotentials and η for the ZS-III scheme of 2-HfS_2^x/$SiSe^y$.

Configuration	$x(H_2)$(eV)	$x(O_2)$ (eV)	E_g(HSE)	$\triangle\Phi$(eV)	η(%)
4%	0.83	1.50	2.29	0.08	11.48
3%	0.87	1.38	2.30	0.01	11.41
2%	0.92	1.33	2.31	0.10	11.07
1%	0.96	1.27	2.33	0.19	10.67
0	1.01	1.19	2.35	0.27	10.20
-1%	1.06	1.11	2.37	0.36	9.83
-2%	1.11	1.02	2.39	0.44	9.41
-3%	1.19	0.92	2.44	0.53	8.65

Table S10 The overpotentials and η for the ZS-IV scheme of 2-HfS_2^x/$SiSe^y$.

Configuration	$x(H_2)$(eV)	$x(O_2)$ (eV)	E_g(HSE)	$\triangle\Phi$(eV)	η(%)
4%	0.90	1.58	2.29	0.08	11.48
3%	0.86	1.37	2.30	0.01	11.41
2%	0.82	1.24	2.31	0.10	11.07
1%	0.78	1.08	2.33	0.19	10.67
0	0.74	0.92	2.35	0.27	10.20
-1%	0.70	0.75	2.37	0.36	9.83
-2%	0.67	0.57	2.39	0.44	8.99
-3%	0.66	0.39	2.44	0.53	5.78

Table S11 The overpotentials and η for the ZS-I scheme of 3-HfS_2^x/$SiSe^x$.

Configuration	$x(H_2)$(eV)	$x(O_2)$ (eV)	E_g(HSE)	$\triangle\Phi$(eV)	η(%)
4%	0.91	1.48	2.40	0.06	9.56
3%	0.89	1.37	2.42	0.01	9.29
2%	0.89	1.29	2.45	0.05	8.80
1%	0.83	1.24	2.47	0.15	8.37
0	0.81	1.16	2.50	0.22	7.89
-1%	0.80	1.08	2.55	0.29	7.22
-2%	0.79	0.98	2.58	0.35	6.79
-3%	0.77	0.88	2.62	0.42	6.28

Table S12 The overpotentials and η for the ZS-II scheme of 3-HfS_2^x/$SiSe^x$.

Configuration	$x(H_2)$(eV)	$x(O_2)$ (eV)	E_g(HSE)	$\triangle\Phi$(eV)	η(%)
4%	0.85	1.54	2.40	0.06	9.56
3%	0.89	1.37	2.42	0.01	9.29
2%	0.94	1.24	2.45	0.05	8.80
1%	0.98	1.10	2.47	0.15	8.37
0	1.03	0.95	2.50	0.22	7.89
-1%	1.09	0.79	2.55	0.29	7.22
-2%	1.14	0.63	2.58	0.35	6.79
-3%	1.19	0.46	2.62	0.42	4.77

Table S13 The overpotentials and η for the ZS-III scheme of 3-HfS_2^x/$SiSe^x$.

Configuration	$x(H_2)$(eV)	$x(O_2)$ (eV)	E_g(HSE)	$\triangle\Phi$(eV)	η(%)
4%	0.85	1.48	2.40	0.06	9.56
3%	0.89	1.37	2.42	0.01	9.29
2%	0.94	1.29	2.45	0.05	8.80
1%	0.98	1.24	2.47	0.15	8.37
0	1.03	1.16	2.50	0.22	7.89
-1%	1.09	1.08	2.55	0.29	7.22
-2%	1.14	0.98	2.58	0.35	6.79
-3%	1.19	0.88	2.62	0.42	6.28

Table S14 The overpotentials and η for the ZS-IV scheme of 3-HfS_2^x/$SiSe^x$.

Configuration	$x(H_2)$(eV)	$x(O_2)$ (eV)	E_g(HSE)	$\triangle\Phi$(eV)	η(%)
4%	0.91	1.54	2.40	0.06	9.56
3%	0.89	1.37	2.42	0.01	9.29
2%	0.89	1.24	2.45	0.05	8.80
1%	0.83	1.10	2.47	0.15	8.37
0	0.81	0.95	2.50	0.22	7.89
-1%	0.80	0.79	2.55	0.29	7.22
-2%	0.79	0.63	2.58	0.35	6.79
-3%	0.77	0.46	2.62	0.42	4.70

References

1. M. Faghihnasiri, A. Ahmadi, S. A. Golpayegan, S. G. Sharifabadi and A. Ramazani, *Nanomaterials*, 2020, **10**.
2. H. C. Lu, Y. Z. Guo and J. Robertson, *Appl. Phys. Lett.*, 2018, **112**.
3. D. Singh and R. Ahuja, *ACS Appl. Energ. Mater.*, 2019, **2**, 6891-6903.
4. M. Salavati, *Front. Struct. Civ. Eng.*, 2019, **13**, 486-494.
5. B. Wang, X. Wang, P. Wang, T. Yang, H. Yuan, G. Wang and H. Chen, *Nanomaterials*, 2019, **9**, 1706.
6. C. Kamal, A. Chakrabarti and M. Ezawa, *Phys. Rev. B*, 2016, **93**, 125428.
7. S. P. Poudel and S. Barraza-Lopez, *Phys. Rev. B*, 2021, **103**, 024107.
8. J. Bardeen and W. Shockley, *Phys. Rev.*, 1950, **80**, 72.
9. C. F. Fu, J. Y. Sun, Q. Q. Luo, X. X. Li, W. Hu and J. L. Yang, *Nano Lett.*, 2018, **18**, 6312-6317.